

# Scaling of excitations in dimerized and frustrated spin-1/2 chains

D. Controzzi,<sup>1</sup> C. Degli Esposti Boschi,<sup>2</sup> F. Ortolani,<sup>3,2</sup> and S. Pasini<sup>3</sup>

<sup>1</sup>International School for Advanced Studies and INFN, Via Beirut, 1, 34100, Trieste, Italy

<sup>2</sup>CNR-INFN, Research Unit of Bologna, Viale Berti-Pichat, 6/2, 40127, Bologna, Italy

<sup>3</sup>Physics Department, University of Bologna and INFN, Viale Berti-Pichat, 6/2, 40127, Bologna, Italy

We study the finite-size behavior of the low-lying excitations of spin-1/2 Heisenberg chains with dimerization and next-to-nearest neighbors interaction,  $J_2$ . The numerical analysis, performed using density-matrix renormalization group, confirms previous exact diagonalization results and shows that, for different values of the dimerization parameter  $\delta$ , the elementary triplet and singlet excitations present a clear scaling behavior in a wide range of  $\ell = L/\xi$  (where  $L$  is the length of the chain and  $\xi$  is the correlation length). At  $J_2 = J_{2c}$ , where no logarithmic corrections are present, we compare the numerical results with finite-size predictions for the sine-Gordon model obtained using Lüscher's theory. For small  $\delta$  we find a very good agreement for  $\ell \gtrsim 4$  or 7 depending on the excitation considered.

PACS numbers: 75.10.Pq, 75.10.Jm, 11.10.Kk, 11.10.St

Spin-1/2 chains with frustration and explicit dimerization have attracted a lot of attention for their experimental relevance to spin-Peierls materials<sup>1</sup> as well as for their interesting theoretical properties, related, for instance, to the presence of two independent mechanisms for spin-gap generation. The difficulties in studying these systems are a consequence of the lack of quantitative analytical methods to describe their full phase diagram and of different types of limitations in the currently available numerical methods. On the one hand, with exact diagonalization one can treat at most few dozens of sites, which is inadequate when the correlation length becomes large. On the other, using the density-matrix renormalization group (DMRG) technique<sup>2</sup> it is possible to reach hundreds of sites, but the control on the quantum numbers of the excitations is much more complicated. In both cases it is difficult to reconstruct the infinite-size spectrum in absence of a theory that describes the finite-size effects, especially because some excitations (like the singlet - see below) are known to have a *non-monotonic* dependence on the chain length  $L$  (Ref. 3). In this paper we present a detailed finite-size analysis of DMRG results for the low-energy excitations of a spin-1/2 chain with frustration and explicit dimerization, with the aim of getting a deeper theoretical understanding of the corrections due to finite  $L$ . In particular, along a specific line in parameter space, where the spin chain is described by a massive integrable quantum field theory (QFT), we compare the numerical results with analytical predictions for the finite-size scaling based on Lüscher's theory<sup>4,5</sup>.

The Hamiltonian of a frustrated spin-1/2 chain with explicit dimerization has the standard form

$$H = J \sum_{i=1}^L [(1 + (-)^i \delta)] \mathbf{S}_i \cdot \mathbf{S}_{i+1} + J_2 \sum_{i=1}^L \mathbf{S}_i \cdot \mathbf{S}_{i+2} \quad (1)$$

(periodic boundary conditions are assumed in the following). For  $\delta = 0$  one identifies two regimes. For  $J_2 < J_{2c} \cong 0.24J$  the model is gapless and described, at low energies, by the  $SU(2)$  Wess-Zumino-Witten-

Novikov (WZWN) conformal field theory at level  $k = 1$  ( $SU(2)_1$ ), with a marginally irrelevant perturbation. When  $J_2 > J_{2c}$  the marginal perturbation changes sign and induces a gap in the spectrum. In terms of operators of the WZWN theory the dimerization term is proportional to the trace of the  $SU(2)$  matrix field  $g$ . Then, in the low energy limit, (1) is described by the following Hamiltonian density<sup>6,7</sup>

$$\mathcal{H} = \mathcal{H}_{SU(2)_1} - \gamma \bar{\mathbf{J}} \cdot \mathbf{J} + \eta \text{Tr}g, \quad (2)$$

where  $\mathcal{H}_{SU(2)_1} = \frac{2\pi v}{3} [:\mathbf{J} \cdot \mathbf{J}: + :\bar{\mathbf{J}} \cdot \bar{\mathbf{J}}:]$ ,  $\mathbf{J}$  and  $\bar{\mathbf{J}}$  are the chiral  $SU(2)$  currents and satisfy the level  $k = 1$  Kac-Moody algebra. The coupling constants are linearly related to  $J_2$  and  $\delta$ :  $\gamma \propto (1 - J_2/J_{2c})$  and  $\eta \propto \delta$ . It should always be kept in mind that, roughly speaking, the field theory description is valid if the masses are much smaller than the bandwidth, that implies  $\delta \ll 1$  or, for  $\delta = 0$ ,  $(J_2 - J_{2c})/J \ll 1$ .

The theory (2) is integrable when one of the two coupling constants vanish. For  $\eta = 0$  excitations are massive (massless) spinons for  $\gamma < 0$  ( $\gamma > 0$ ). When  $\eta \neq 0$ , the strongly relevant perturbation  $\text{Tr}g$  introduces a confining interaction between the spinons that are no longer fundamental excitations of (2)<sup>8,9</sup>. For  $\gamma = 0$  the model is again integrable and equivalent to the sine-Gordon (SG) model,  $\mathcal{L} = 1/2(\partial_\mu \varphi)^2 - g_1/(2\pi^2 v) \cos(\beta\varphi)$ , at  $\beta^2 = 2\pi$ , and the spectrum contains triplet and singlet excitations<sup>7,10</sup>. The ratio between their masses,  $R = m_s/m_t$ , is known exactly to be  $R = \sqrt{3}$ .

The behavior of  $R$  for finite values of  $\gamma$  (and  $\eta \neq 0$ ) is difficult to address analytically even in the regime of validity of the field theory description, because (2), like its lattice counterpart (1), is not integrable. This problem was studied using exact diagonalization in Ref. 3, where it was found that the singlet is stable for any  $J_2 < J_{2c}$  and  $R$  interpolates between  $\sqrt{3}$  at  $J_2 = J_{2c}$  and  $R = 2$  at  $J_2 = 0$ . These results are reproduced by our DMRG analysis, although we do not report them here (see however Ref. 11 for the extension to  $J_2 < 0$ ). Some analytical predictions can be made in the vicinity of the two

integrable points, where a perturbative analysis can be carried on<sup>8,9</sup>.

For the analysis of the above problem as well as many others it is essential to have a theory for the finite-size scaling that allows one to extrapolate numerical results. For massive integrable QFTs it is possible to express the leading finite-size corrections to the spectrum in terms of their exact scattering data<sup>4,5</sup>. As we recalled, there are two points for which (2) is integrable. In this paper we consider the integrable point  $\gamma = 0$  and  $\eta \neq 0$ , rather than  $\eta = 0$  and  $\gamma < 0$ , because the former case presents bound states and is physically more interesting. Numerically, this is also the easiest scenario to investigate because in the other case the gap opens very weakly<sup>12</sup>. Hence, in the following we will compare DMRG data for the lattice Hamiltonian (1) with  $J_2 = J_{2c}$  and  $\delta \ll 1$  with predictions coming from the SG theory at  $\beta^2 = 2\pi$ .

Let us start presenting the numerical results. Before studying the finite size-effects we extract from the numerical data some important non-universal pre-factors – a problem recently addressed in Ref. 13. It is well known that, in absence of logarithmic corrections, the triplet mass scales as  $m_t = A_t \delta^{2/3}$ , with  $A_t$  being a non-universal amplitude. The energy gaps, computed with DMRG, are linearly related to the masses through a velocity pre-factor that we express as  $v = C_v J \pi / 2$ :  $\Delta E_t = v m_t$  (the lattice spacing is formally set to one). For  $J_2 = 0$  it is known that  $C_v = 1$ , but for  $J_2 = J_{2c}$  the constant may assume a different value. Another unknown constant connects  $\delta$  with the coefficient of the relevant term in the SG model:  $g_1 = 6J\delta(\pi/2)^{1/4}C_\delta$  ( $C_\delta = 1$  for  $J_2 = 0$ <sup>13</sup>). Along the same lines of Ref. 13 we can extract these constants from the pre-factors of the triplet gap and ground-state energy density, that we write as  $\Delta E_t/J = 1.723K_t\delta^{2/3}$  and  $[e_{GS}(\delta) - e_{GS}(0)]/J = -0.2728K_{GS}\delta^{4/3}$ , respectively. The relation between the constants is  $K_t = C_v (C_\delta/C_v)^{2/3}$  and  $K_{GS} = C_v (C_\delta/C_v)^{4/3}$ . We have computed these quantities for some values of  $\delta$  using the finite-system DMRG algorithm<sup>2</sup> with three “zips” in a range of  $L$  from 10 to 100. The results are presented in Table I, and imply  $C_v \simeq 0.81$  and  $C_\delta \simeq 1.53$  at  $J_2 = J_{2c}$ , to be compared with  $C_\delta = C_v = 1$  at  $J_2 = 0$ .

Let us now come to the central part of the paper by examining the finite-size features of the low-energy spectrum. In the framework of the DMRG this is done by building the superblock density matrix as a mixture (with equal weights) of the matrices associated with a prescribed number of target states. By means of the thick-restart variant of the Lanczos method<sup>14</sup> we are able to target up to ten excited states in each sector of  $S_{\text{tot}}^z = \sum_i S_i^z$ , which is the only good quantum number that we have exploited. First of all from the so-called 1-particle (1P) excitations of the triplet we can get an independent estimate of the velocity. In fact, these excitations for small momenta  $q_n = 2\pi n/L$  (with  $n = \pm 1, \pm 2, \dots$ ) have energy  $E_n = E_{GS} + \sqrt{\Delta E_t^2 + v_1^2 q_n^2}$ . So we have checked that  $L\sqrt{\Delta E_n^2 - \Delta E_t^2}/2\pi$  actually scale as  $nv_1$  and we have reported the values of  $v_1$  in

$\delta$	$\Delta E_t/J$	$K_t$	$K_{GS}$	$v_1/J$	$L_{\min}(\delta)$
0.01	0.09875	1.235	1.966	1.1921	50
0.02	0.15705	1.237	1.948	$1.1822 \pm 0.0010$	30
0.10	0.46233	1.245	1.800	$1.1425 \pm 0.0003$	10

TABLE I: Triplet gaps, constants  $K_t$ ,  $K_{GS}$  and estimates of the “1-particle velocity”  $v_1$  for different values of  $\delta$  and  $J_2 = J_{2c}$  (see text after Eq. (10) for the determination of  $\Delta E_t/J$ ). Typically  $M = 256$  optimized DMRG states have been retained. When  $\Delta E_t < 0.1$  we have improved the precision using  $M = 405$ . The last column contains the (approximate) values at which the singlet gaps attain a minimum.

Table I. Unfortunately, these states with nonzero momentum represent also the main limitation that we have encountered in the computation of the singlet gap  $\Delta E_s$  at large values of  $\delta$ . This is because all the excited states that we can target in  $S_{\text{tot}}^z = 0$ , say  $N_0$ , are eventually exhausted by the triplet and its 1P excitations. In practice, the singlet “disappears” from the set of DMRG levels for  $L \gtrsim (N_0 - 2)\pi v_1 / \Delta E_t \sqrt{R^2 - 1}$ , where  $R$  is the mass ratio<sup>15</sup>. In addition, unlike the triplet, the singlet level has a non-monotonic dependence on  $L$ . Typically  $\Delta E_s(L)$  decreases with increasing  $L$  up to a characteristic value  $L_{\min}(\delta)$ , beyond which it starts to increase and converges to the asymptotic limit *from below*. An example of such a feature is plotted in Fig. 1 for  $\delta = 0.02$  and  $J_2 = J_{2c}$ . As listed in Table I the values of  $L_{\min}$  increase for  $\delta \rightarrow 0$  so that there exists a minimum value of  $\delta$  below which  $L_{\min}$  becomes larger than the maximum reliable size that we can handle with the DMRG.

There are other cases in the literature for which numerical results show that some states in the spectrum exhibit a non-monotonic dependence on  $L$  (see for instance Refs. 16). In such situations it is particularly difficult to get a reliable estimate of the infinite-size value. In some cases it is possible to push  $L$  beyond the minimum and even beyond the flex where the finite-size data start to saturate. Whenever this is not the case the construction of a suitable fitting function becomes essential. In Ref.s 3,17, some empirical scaling functions were suggested that provide a good fit of the numerical data. Nevertheless these expressions were not obtained from a consistent theoretical construction and contain various fitting parameters. In the following we will construct the finite-size corrections using the QFT description. In particular we will compute rigorously the dominant contribution to the scaling functions for large  $L$ . These expressions contain no fitting parameters.

As already recalled for  $J_2 = J_{2c}$  and  $\delta \ll 1$  the spin chain is described by the integrable SG model at  $\beta^2 = 2\pi$ . The factorized scattering theory explicitly shows the hidden  $SU(2)$  symmetry of the model at this point<sup>7</sup>. The spectrum consists of a soliton  $s$  and an anti-soliton  $\bar{s}$  which are degenerate with a breather state  $b_1$ . Moreover, all these particles have the same S-matrix<sup>7,10</sup>

$$S_{a,b}(\theta) = S_0(\theta) = \frac{\sinh \theta + i \sin \pi/3}{\sinh \theta - i \sin \pi/3}, \quad a, b = s, \bar{s}, b_1. \quad (3)$$

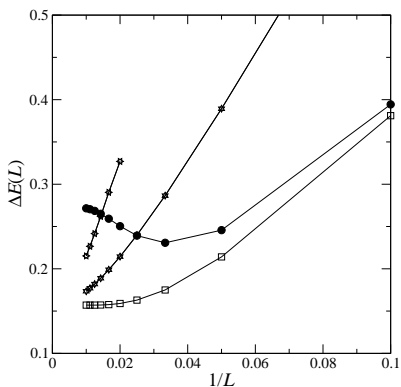


FIG. 1: Finite-size gaps vs  $1/L$  for  $\delta = 0.02$  and  $J_2 = J_{2c}$ : triplet (open squares), singlet (full circles), lowest 1P triplet excitations with momenta different from  $0$  and  $\pi$  (coinciding up and down triangles). Following the singlet at large  $L$  requires to target various excited states within  $S_{\text{tot}}^z = 0$  ( $N_0 = 6$  in this example, where  $M = 256$ ), due to the crossing with 1P states. The singlet curve has a minimum at  $L_{\text{min}}(0.02) \simeq 30$ .

The rapidity  $\theta$  parameterizes the relativistic dispersion relations:  $e_a = m_a \cosh \theta$ ,  $p_a = m_a \sinh \theta$ . In addition, there is another breather state  $b_2$  of higher mass. The additional S-matrices are<sup>7,10</sup>

$$S_{a,b_2}(\theta) = S_0(\theta + i\pi/6)S_0(\theta - i\pi/6), \quad a = s, \bar{s}, b_1; \quad (4)$$

$$S_{b_2,b_2}(\theta) = [S_0(\theta)]^3. \quad (5)$$

The excitations can be then organized into a triplet  $(s, \bar{s}, b_1)$  of mass  $m_t$  and a singlet of mass  $m_s = \sqrt{3}m_t$ .

For what follows, it is worth recalling that bound states, like the breathers, are associated to poles in the S-matrix. In particular if  $\theta = iu_{bc}^a$  is a pole in the scattering process of the particle  $b$  and  $c$  the mass of the bound state is given by:  $m_a^2 = m_b^2 + m_c^2 + 2m_b m_c \cos u_{bc}^a$ . For instance, the simple poles in the S-matrix  $S_{s,\bar{s}}(\theta)$  at  $\theta = 2i\pi/3$  and  $\theta = i\pi/3$  correspond to the two breathers (it is easy to check their masses are  $m_t$  and  $m_s$  respectively). The third order pole at  $\theta = 2\pi i/3$  in  $S_{b_2,b_2}(\theta)$  should be interpreted as associated to intermediate virtual particles in the scattering processes<sup>18</sup>, as drawn in Fig. 2. All other poles in (3-5) are redundant and do not correspond to additional bound states<sup>10</sup>.

The finite-size corrections for a QFT in a large but finite volume with periodic boundary conditions are a consequence of the vacuum polarization and, when the model is integrable, they can be extracted from the exact scattering data of the infinite-volume theory<sup>4,5</sup>. The leading corrections to the masses are exponentially small and consist of two terms

$$\Delta m_a(L) = \Delta m_a^{(F)}(L) + \Delta m_a^{(\mu)}(L), \quad (6)$$

which roughly can be understood as follows. The first term exists in any theory and can be interpreted as virtual particles “traveling around the world” once before

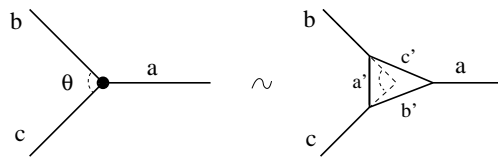


FIG. 2: Physical interpretation of third order poles. The angle  $\theta$  is related to the poles in the intermediate processes as  $\theta = u_{b,a'}^{c'} + u_{c,a'}^{b'} - \pi$ .

being annihilated again. It has the form

$$\Delta m_a^{(F)}(L) = - \sum_b \int_{-\infty}^{\infty} \frac{d\theta}{2\pi} e^{-e_b(\theta)L} e_b(\theta) f_{a,b}(\theta), \quad (7)$$

where  $f_{a,b}(\theta) = S_{a,b}(\theta + \frac{i\pi}{2}) - 1$ . For large  $L$  Eq. (7) is of order  $\mathcal{O}(e^{-m_b L})$ . The second term in (6) is present only in theories with bound states and is associated to virtual processes in which a particle is split into its two constituents that “travel around the world” before recombining again into the original particle. If the particle  $a$  is bound state of two other particles of the theory, say  $b, c$ , associated to the pole  $\theta = iu_{bc}^a$ , then  $\Delta m_a^{(\mu)}(L)$  reads

$$\Delta m_a^{(\mu)}(L) = - \sum_{b,c} \Theta(m_a^2 - |m_b^2 - m_c^2|) \mu_{abc} R_{abc} e^{-\mu_{abc} L}, \quad (8)$$

where  $\Theta$  denotes the Heaviside step function and

$$\mu_{abc} = m_b \sin u_{ab}^c, \quad R_{abc} = -i \text{Res}_{\theta=i u_{ab}^c} S_{a,b}(\theta). \quad (9)$$

As mentioned before the third order pole has to be interpreted as formation of virtual particles and  $R_{abc} = R_{ab'c'} R_{ba'c'} R_{cb'a'}$ . In general, since for small  $L$ ,  $\Delta E_{s,t}(L) \sim 1/L$ , if the terms above approach the infinite-volume limit from below the scaling function will present a minimum (the minimum may also appear as a consequence of the competition of the two terms in (6)<sup>5</sup>).

Since the singlet and the triplet masses are related, all the finite-size corrections depend on the scaling variable  $m_t L$  (Ref. 19). Using formulas (6-8) and the pole structure of the S-matrix, we find the following expression for the leading finite-size corrections,  $\Phi_{s,t}(\ell) \equiv \Delta E_{s,t}(L)/\Delta E_t(\infty)$ ,

$$\Phi_t(\ell) = 1 + 6e^{-\ell\sqrt{3}/2} - 3 \int_{-\infty}^{\infty} \frac{d\theta}{2\pi} e^{-\ell \cosh \theta} f_0(\theta), \quad (10)$$

$$\Phi_s(\ell) = \sqrt{3} \left( 1 - 3e^{-\ell/2} - 36e^{3\ell/2} \right), \quad (11)$$

with  $f_0(\theta) \equiv 2\sqrt{3} \cosh \theta / (2 \cosh \theta - \sqrt{3})$ . These scaling functions are compared to the scaled DMRG data in Fig. 3a (one has to replace  $m_t L$  with the scaling variable  $\ell = L/\xi$ ). For each value of  $\delta$  the scale factors  $\xi$  (slightly different for triplet and the singlet) and  $\Delta E_t$  have been tuned in order to give the best collapse of the curves. Using the numbers found for the triplet, the product  $v = \xi \Delta E_t$  yields another estimate of the velocity,  $v = 1.19 \pm 0.01$ , in agreement with those in Table I.

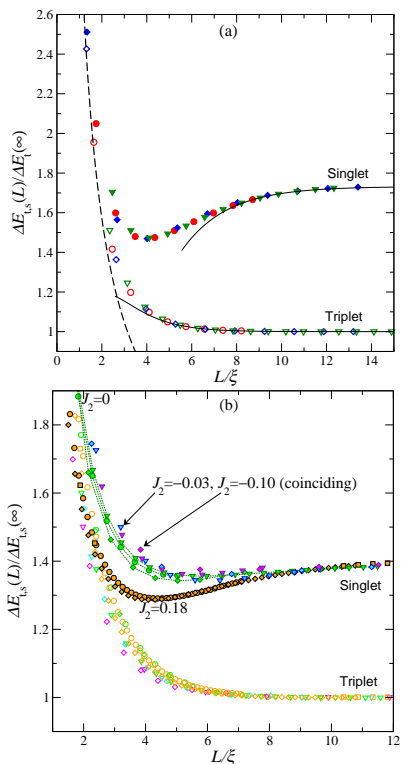


FIG. 3: (a) Scaling plot of finite-size corrections to the triplet and singlet gaps  $\Delta E_{t,s}(L)$  at  $J_2 = J_{2c}$ . Continuous lines represent the analytical predictions (10) and (11), while the symbols refer to DMRG data obtained with the same parameters as in Table I (circles:  $\delta = 0.01$ ; diamonds:  $\delta = 0.02$ ; triangles:  $\delta = 0.10$ ). The dashed line shows the  $1/\ell$  behavior at small  $\ell$ . (b) Same as in (a) for  $J_2 < J_{2c}$  ( $\delta = 0.06$ ). The singlet data have been rescaled by  $\Delta E_s(\infty)$  and then shifted by  $+0.4$  for clarity reasons.

A first interesting result of this analysis is that stable excitations of the lattice model for  $J_2 = J_{2c}$  with a dimerization term exhibit a clear scaling behavior over the whole range of  $L$  for different values of  $\delta$ . Moreover, the scaling functions obtained using the QFT description capture well the finite-size effects of the spin Hamiltonian for  $\ell \gtrsim 4$  or  $7$ , depending on which of the two excitations we consider. We recall that the analytic results are the exact expression of the leading finite-size corrections and contain no additional fitting parameters.

Finally, we have repeated the numerical analysis for other values of  $J_2$ . Unfortunately in this case the low-energy effective field theory is no longer integrable and computations of finite-size corrections are much more difficult. In principle both the variation of the mass and of the S-matrix can be taken into account perturbatively<sup>20</sup>. The numerical results are reported in Fig. 3b. We note that the form of the scaling function for the singlet has a much stronger dependence on  $J_2$  than the triplet one. For fixed  $J_2$  we find again no appreciable dependence on  $\delta$ .

We would like to thank G. Mussardo for suggesting to compare the DMRG results with Lüscher's theory and for essential discussions. D.C. thanks A. Nersisyan for important discussions and interest in the work. We also acknowledge useful observations made by E. Ercolessi, G. Morandi, M. Roncaglia, L. Campos Venuti and G. Delfino. This work was partially supported by the TMR network EUCLID (HPRN-CT-2002-00325), and by the Italian MIUR through COFIN projects (prot. n. 2002024522\_001 and 2003029498\_013).

<sup>1</sup> M. Aïn *et al.*, Phys. Rev. Lett. **78**, 1560 (1997); M. Weiden *et al.*, Z. Phys. B **103**, 1 (1997); M. Fischer *et al.*, Phys. Rev. B **60**, 7824 (1999).  
<sup>2</sup> S. R. White, Phys. Rev. B **48**, 10345 (1993).  
<sup>3</sup> G. Bouzerar, A. P. Kampf and G. I. Japaridze, Phys. Rev. B **58**, 3117 (1998).  
<sup>4</sup> M. Lüscher, Comm. Math. Phys. **104**, 177 (1986).  
<sup>5</sup> T. R. Klassen and E. Melzer, Nucl. Phys. B **362**, 329 (1991); V.P. Yurov, A.B. Zamolodchikov, Int. J. Mod. Phys. A **5**, 3221 (1990).  
<sup>6</sup> I. Affleck and F. D. M. Haldane, Phys. Rev. B **36**, 5291 (1987).  
<sup>7</sup> I. Affleck, Nucl. Phys. B **265**, 448 (1986).  
<sup>8</sup> I. Affleck, in *Dynamical properties of unconventional magnetic systems*, Kluwer Academic Publishers (1997) and cond-mat/9705127.  
<sup>9</sup> D. Controzzi and G. Mussardo, Phys. Rev. Lett. **92**, 021601 (2004); Phys. Lett. B **617**, 133 (2005).  
<sup>10</sup> A. B. Zamolodchikov and Al. B. Zamolodchikov, Ann. Phys. NY **120**, 253 (1979).  
<sup>11</sup> L. Campos Venuti *et al.*, J. Stat. Mech. (2005), L02004.  
<sup>12</sup> R. Chitra *et al.*, Phys. Rev. B **52**, 6581 (1995).  
<sup>13</sup> E. Orignac, Eur. Phys. J. B **39**, 335 (2004).

<sup>14</sup> For the original algorithm see: K. Wu and H. Simon, SIAM J. Matrix Anal. Appl. **22**, 602 (2000); For the implementation into the DMRG see: C. Degli Esposti Boschi and F. Ortolani, Eur. Phys. J. B **41**, 503 (2004).  
<sup>15</sup> This formula stems from equating  $\Delta E_s = R\Delta E_t$  to the energy of the highest 1P state with momentum  $|q| = 2\pi/L(N_0 - 2)/2$ , given that within the  $N_0$  states we have to include the singlet, the triplet and all the 1P excitations that are doubly degenerate in momentum.  
<sup>16</sup> J. Z. Zhao, *et al.*, Phys. Rev. Lett. **90**, 207204 (2003); J. Lou *et al.*, Phys. Rev. B **68**, 045110 (2003).  
<sup>17</sup> T. Barnes *et al.*, Phys. Rev. B **47**, 3196 (1993).  
<sup>18</sup> S. Coleman and H. J. Thun, Comm. Math. Phys. **61**, 31 (1986); C. J. Goebel, Progr. Th. Phys. Suppl. **86**, 261 (1986).  
<sup>19</sup> It should be noticed that the integrals in (7) involving  $f_{a,b2}(\theta)$ , with  $a$  belonging to the triplet, diverge and need to be regularized. Such divergences are possible in one dimensional models, but there is no general prescription to treat them<sup>5</sup>. We regularized them by simply subtracting the divergent part. In any case, it turns out that the contribution from this term (not shown below) is very small and then the choice of the regularization scheme does not

affect the analysis.

<sup>20</sup> G. Delfino, G. Mussardo and P. Simonetti, Nucl. Phys.

**473**, 469 (1996).